Characterizing the South Atlantic Bight seasonal variability and cold-water event in 2003 using a daily cloud-free SST and chlorophyll analysis

Travis N. Miles,[1] Ruoying He,[1] and Mingkui Li[1]

Received 20 October 2008; accepted 9 December 2008; published 22 January 2009.

[1] Concurrent MODIS sea surface temperature (SST) and chlorophyll-a (Chl-a) data are used with a new technique: Data Interpolating Empirical Orthogonal Function (DINEOF) method to produce daily, 4-km, cloud-free SST and Chl-a analyses for the South Atlantic Bight in 2003. Comparisons between SST analysis and in situ buoy temperature demonstrate the utility of DINEOF. To quantify linkages between surface wind, SST, and Chl-a variations, Empirical Orthogonal Function (EOF) analysis is applied to North American Regional Reanalysis winds, and cloud-free DINEOF SST and Chl-a analyses. Wind EOF modes highlight upwelling winds from June to September. While the first SST mode represents seasonal heat flux variations, the second SST mode shows a direct response to upwelling winds with an abrupt drop in SST. The top two Chl-a EOF modes show less connection with wind. More subsurface Chl-a and nutrient observations are needed to quantify its relation with surface wind. **Citation:** Miles, T. N., R. He, and M. Li (2009), Characterizing the South Atlantic Bight seasonal variability and cold-water event in 2003 using a daily cloud-free SST and chlorophyll analysis, *Geophys. Res. Lett.*, *36*, L02604, doi:10.1029/2008GL036396.

1. Introduction

[2] The South Atlantic Bight (SAB) is a highly variable coastal ocean system that can be separated dynamically into the inner, middle, and outer shelves [*Atkinson*, 1985]. The SAB inner shelf (0-20 m) is forced by river runoff and local winds; the middle shelf (20-40 m) is forced by local winds and Gulf Stream (GS) intrusions; and the outer shelf (40-70 m) is forced by GS, eddies, and meanders [e.g., *Lee et al.*, 1991]. Such distinctions in cross-shelf forcing mechanisms, along with other factors such as isobath divergence in the Straits of Florida, isobath convergence off the Carolinas, the semi-permanent gyre created by the Charleston Bump, and locations of the Gulf Stream Front lead to complex spatial and temporal distributions of ocean physical and biological properties in the SAB, as manifested by satellite observed sea surface temperature (SST) and chlorophyll-a (Chl-a) color imagery [e.g., *Yoder*, 1985; *Signorini and McClain*, 2006, 2007].

[3] During the summer of 2003, an anomalous cold-water event took place in the central SAB. Early studies [*Aretxabaleta et al.*, 2006, 2007; *Yuan*, 2006] have shown that anomalously large precipitation and river discharge were present along the Southeastern Continental Shelf during that time, producing a strong stratification with a shallow thermocline. From June to mid-July, persistent southwesterly winds elevated the thermocline and produced intensive upwelling along the SAB. This upwelling event lasted into September, when the passage of an atmospheric front on September 7-8 2003 terminated the southwesterly winds. Both *Aretxabaleta et al.* [2006] and *Yuan* [2006] presented in situ hydrography and remote sensing observations to document this cold-water event. While offering valuable dynamics insights, these studies only used monthly-composite and selected low-cloud coverage SST and Chl-a snapshots, thus limiting our understanding of short-term SST and ocean color variations during this cold-water event in the context of the seasonal evolution in 2003.

[4] We present here a new daily, high-resolution, cloud-free SST and Chl-a analysis for the SAB using the Data Interpolating Empirical Orthogonal Function (DINEOF) method [*Alvera-Azcarate et al.*, 2007]. This new analysis technique provides an accurate space and time reconstruction of otherwise cloud-covered SST and Chl-a fields. Compared with a traditional optimal interpolation (OI) method, such as that used by *He et al.* [2003], DINEOF is highly efficient for processing of large datasets. It does not require a priori temporal and spatial decorrelation scales, which are not readily available for a dynamically complex coastal ocean, such as the SAB. We begin in Section 2 with a description of satellite and wind data used in this study. Section 3 outlines the DINEOF procedure for generating daily cloud-free SST and chlorophyll analysis, as well as their validations. Empirical Orthogonal Function (EOF) analysis is applied in Section 4 to characterize the SAB seasonal variability and the cold-water event in the summer of 2003, followed by a summary and conclusion in Section 5.

2. Data

[5] The Moderate Resolution Imaging Spectroradiometer (MODIS) daily SST and Chl-a data are utilized in this study. The MODIS sensor was launched in 2002 aboard the sun-synchronous polar orbiting satellite Aqua. MODIS is only capable of viewing in the visible and infrared wave bands, thus almost all images have cloud cover to various extents. A major advantage of the MODIS sensor is that it is of sufficiently high resolution to resolve fine-scale structures in the ocean. Moreover, SST and Chl-a are measured concurrently for the first time, allowing for 1) examination of the covariations of SST and Chl-a; and 2) enhanced correlation between variables when using the multivariate DINEOF procedure described in Section 3.

[1]Department of Marine, Earth and Atmospheric Sciences, North Carolina State University, Raleigh, North Carolina, USA.

0094-8276/09/2008GL036396$05.00

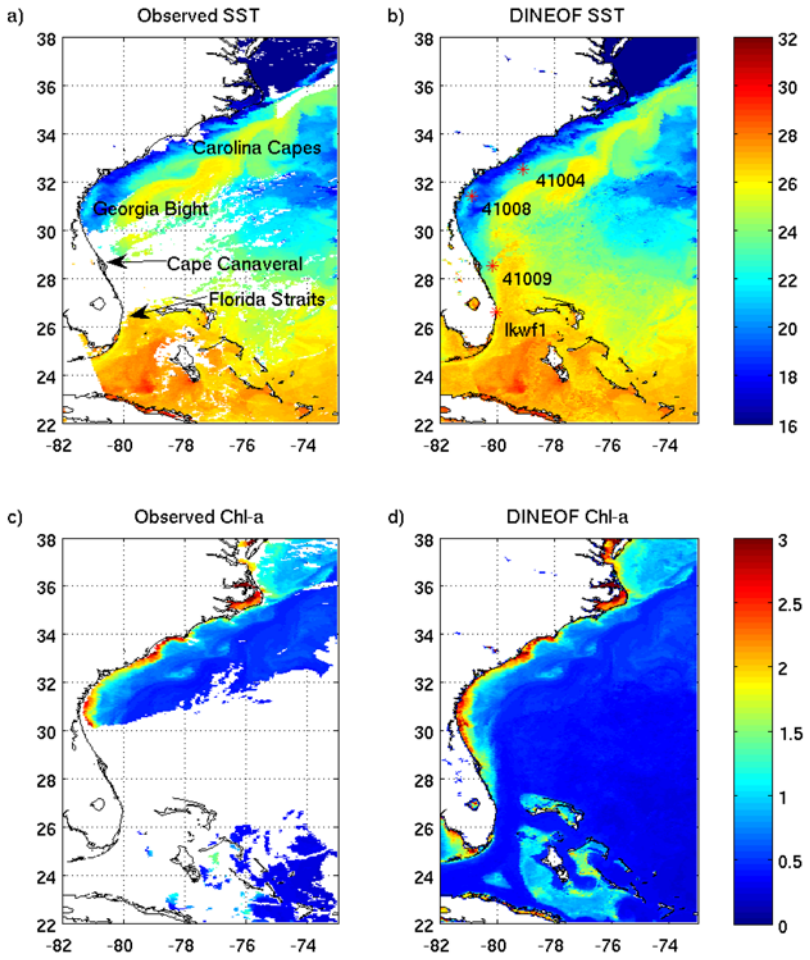

Figure 1. Examples of Raw MODIS (a) SST and (c) chlorophyll and their DINEOF (b) SST and (d) chlorophyll reconstructions on March 22nd, 2003. Figure 1a contains geographic references, and Figure 1b indicates buoy validation locations.

[6] Both SST and Chl-a products are gridded Level 3 fields collected from the National Aeronautics and Space Administration (NASA) Goddard Space Flight Center (GSFC). Level 3 data were collected from January 1, 2003 to December 31, 2003 in a 4-km resolution 384 × 215 pixel grid ranging from 22°N to 38°N latitude and 73°W to 82°W longitude. Given that data with over 95% cloud contamination cannot be accurately reconstructed with the DINEOF method [*Alvera-Azcarate et al.*, 2005], we removed days where chlorophyll cloud contamination exceeded 95% from both the SST and Chl-a datasets (Chl-a traditionally has greater cloud cover) to ensure input data quality. Of the initial 365 days, 295 were retained for analysis.

[7] To characterize surface wind conditions, we also utilized wind fields provided by the National Centers for Environmental Protection (NCEP) North American Regional Reanalysis (NARR, http://www.cdc.noaa.gov/). NARR products are derived from the NCEP data-assimilative atmospheric model at 3-hour temporal resolution and 32-km spatial resolution. We sampled only noon surface winds for 2003, resulting in 365 daily wind fields on the same domain as SST and Chl-a.

[8] For the purpose of validating our DINEOF analysis, in situ temperature data from buoys 41004, 41008, 41009, and lkwf1 (Figure 1b) were downloaded from the National Data Buoy Center (NDBC) website http://www.ndbc.noaa.gov/). Buoy data are collected hourly and we computed their daily means for comparison with reconstructed satellite fields.

3. Method

[9] We present here a concise description of the DINEOF procedure. Interested readers are referred to *Alvera-Azcarate et al.* [2007] for more details. First, the initial data input (X) is obtained by subtracting of the temporal mean and setting the missing data to 0. Second, a Singular Value Decomposition (SVD) of X is performed, which fills in missing data with a best guess by the equation: $X_{i,j} = \sum_{p=1}^{k} \rho_p (u_p)_i (v_p^T) j$, where i and j in X are the temporal and spatial indexes, respectively, k is the number of EOF modes, $\mathbf{u}_p$ and $\mathbf{v}_p$ are the pth column of the spatial and temporal functions of EOF, and ρ_p (where p = 1. . .k) represents the corresponding singular values. Step 2 is repeated iteratively k times or until convergence, using the previous best guess as the initial value for the subsequent iteration, where convergence is defined by a preset threshold of the absolute value of the difference between the SVD of the current and previous iterations. Third, a cross-validation

Table 1. Point Comparisons of Buoy Observations With Corresponding DINEOF SST and Raw MODIS SST

Buoy	Number of Observations	Mean Offsets	OBS/DINEOF SST Correlations Seasonal Cycle Retained/Removed	OBS/MODIS Raw SST Correlations Seasonal Cycle Retained/Removed
41004	331	−0.18	0.96/0.67	0.97/0.79
41008	365	−0.18	0.99/0.81	0.99/0.84
41009	339	−0.22	0.93/0.59	0.91/0.56
Lkwf1	362	−0.77	0.96/0.57	0.96/0.58

technique determines the optimum number of EOF modes retained in the reconstruction. Finally, the first and second steps are repeated using only the optimum number of EOF modes and the temporal mean is added to the reconstructed matrix to obtain the interpolated dataset.

[10] Following *Alvera-Azcarate et al.* [2007], we used a multivariate adaptation of DINEOF in this study. An extended matrix X_e, which contains multiple state variables, is used in the reconstruction. Specifically, we utilized concurrent SST, Chl-a and 1-day-lagged SST to reconstruct SST fields. Similarly, Chl-a, SST and 1-day-lagged Chl-a are used to reconstruct Chl-a fields. To yield the best reconstruction results, lag time must be determined through sensitivity experiments. We found 1-day lag to be ideal for our purposes. In the event that the following day has less than 5% data coverage the next closest valid day is utilized as the 1-day-lagged data. Correlation between variables is calculated internally and no a priori knowledge of these relationships is necessary to perform the multivariate reconstruction. After reconstruction, only missing (cloud covered) data is filled in and original valid data are retained. Figure 1, as an example, demonstrates DINEOF's ability to construct time and space continuous SST and Chl-a fields.

[11] While no in situ Chl-a data are available for comparison, the DINEOF daily SST reconstruction is validated through direct comparisons with daily-averaged in situ temperature from the four buoys mentioned prior. Statistics (Table 1) show that with the seasonal cycle retained, correlation coefficients are above 0.93 with mean offsets less than 0.77°C at all stations. When the seasonal cycle is removed using the least square harmonic analysis of buoy and DINEOF data independently, correlation coefficients at subseasonal scales are also significant, ranging from 0.57 to 0.81. Differences between DINEOF SST and in situ buoy-measured SST are due to a number of factors including errors in the MODIS retrievals, spatial offsets between buoy locations and the DINEOF SST 4-km footprint and differences between satellite-derived ocean skin temperature and buoy bulk temperature measured 1 to 2 meters below the surface. In light of potential errors, the comparison between analysis and in situ data is robust. Consistent with *Alvera-Azcarate et al.* [2005] findings, we note that on the same computing server used for this study, DINEOF is able to produce statistically similar reconstructions up to 30 times faster than the OI method applied by *He et al.* [2003].

4. Analysis of Seasonal Variability and the Summer Cold Event in 2003

[12] DINEOF reconstructions provide time and space continuous daily SST and Chl-a fields, allowing for direct comparisons with high resolution NARR wind fields to understand their intrinsic linkages. We perform EOF analyses on NARR winds, and cloud-free DINEOF SST and Chl-a fields. Prior to EOF analysis, the temporal mean of each variable is removed from the original datasets. The analyses then provide temporal (principal components) and spatial (EOFs) functions derived from their respective anomaly covariance functions. All EOF

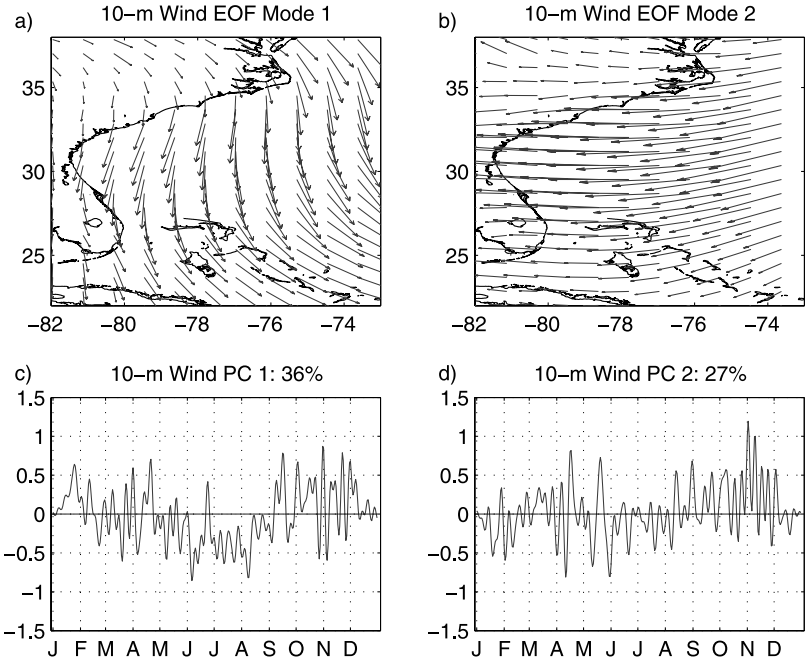

Figure 2. The 2003 NARR wind spatial EOF mode (a) 1 and (b) 2 with their corresponding principal component (PC) (c) 1 and (d) 2. To highlight events with persistence longer than the synoptic scale, the PCs are 7-day low pass filtered.

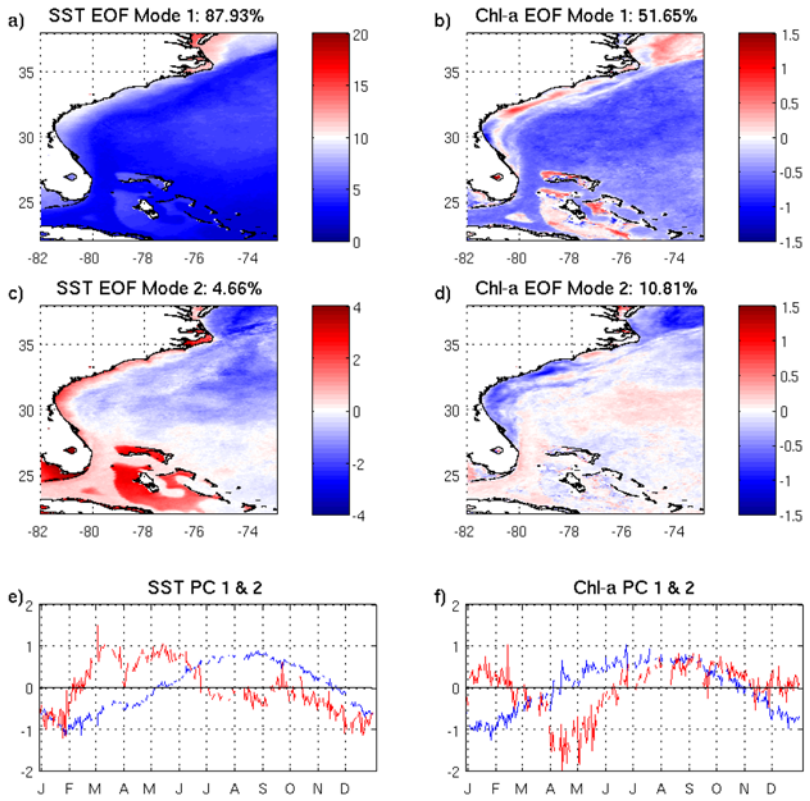

Figure 3. The 2003 reconstructed SST spatial EOF mode (a) 1 and (c) 2 and (e) corresponding principal component 1 (blue) and 2 (red), along with 2003 reconstructed Chl-a spatial EOF mode (b) 1 and (d) 2 and (f) corresponding principal component 1 (blue) and 2 (red). Chl-a is on a natural log scale therefore negative values represent decimals and positive values represent Chl-a greater than 1. Also shown in green is the 200-m contour line.

results have been scaled for better illustration. Chl-a input data is the natural logarithm of Chl-a, therefore results below 0 are equivalent to values between 0 and 1, and results above 0 are equivalent to values above 1.

[13] To highlight events with persistence longer than the synoptic scale, the principal components of surface wind underwent 7-day low-pass filtering. The first wind EOF mode (36% of the variance) (Figures 2a and 2c) shows highly variable wind speed and direction from January to May, which then becomes uniformly northward (upwelling favorable) from June throughout the summer, until a well-defined shift of northward to southward wind occurs in September. The second wind EOF mode (27% of the variance) (Figures 2b and 2d) indicates winds become consistently offshore (upwelling favorable) from June to August, followed by a direction reversal in September, with persistent and strong onshore winds for the remainder of the year. A complete reconstruction of surface wind fields requires more higher-order EOF modes, which together account for another 37% of variance in the wind signal. The fact that each of the top 2 modes shows persistent upwelling-favorable conditions from late spring throughout the summer indicates surface wind plays a major role in strong summer upwelling in 2003. Large-scale wind patterns on the SAB are governed by the Ohio Valley High and the Bermuda-Azores High [*Blanton et al.*, 1985]. *Schwing and Pickett* [2004] suggested the persistent wind pattern in summer 2003 was related to anomalous proximity, size and strength of the Bermuda-Azores High.

[14] The first SST EOF (87.93%) (Figures 3a and 3e) captures the ocean response to the seasonal solar heating cycle. *He and Weisberg* [2003] show that over the seasonal time scale, shallow coastal ocean temperature variation can be expressed by a one-dimensional balance: $\partial T/\partial t = Q/(\rho C_p H)$, where Q is net surface heat flux, ρ the water density, C_p the water specific heat, and H the local water depth. As such, SST variability is inversely proportional to the water depth, and the largest variability with the highest (lowest) water temperature in summer (winter) is seen on the inner shelf. In contrast, temperatures in the offshore GS region stay fairly consistent throughout the year due to both increased water depth and strong heat advection supplied from the tropical ocean.

[15] The second SST EOF mode (4.66%) (Figures 3c and 3e) is more complex, showing the sub-seasonal temperature variations in response to water stratification and wind forcing. In 2003, anomalous precipitation elevated freshwater input to the shelf, creating a strong salinity front and stratification that decoupled the thermocline from the bottom boundary layer [*Yuan*, 2006; *Aretxabaleta et al.*, 2006]. Thermal heating further enhanced the stratification until persistent upwelling winds initiated in June. This caused onshore transport of cold subsurface water, and subsequently a continued drop in SST, as clearly seen in the second mode principal component from June to September.

[16] Spatial variability in Chl-a is apparent in the first and second EOF modes. The first mode (51.65% of the variance)

(Figures 3b and 3f) has trends that are distinctly out of phase for different regions on the SAB. The inner shelf region of the Georgia Bight has decreasing Chl-a concentrations in the spring and increasing concentrations in the fall toward winter. The trend is opposite north of this region along the coast of the Carolinas, where Chl-a concentrations increase in summer months and decrease into winter months. We note such a regional contrast is consistent with earlier findings [e.g., *McClain et al.*, 1984].

[17] The second Chl-a EOF (10.81%) (Figures 3d and 3f) shows more coherent distribution. A regional difference can still be discerned where the Georgia Bight is independent of other coastal and offshore waters. The Georgia Bight region has a major Chl-a peak throughout spring, which coincides with times of increased precipitation and river discharge. In particular, what appears to be a river plume structure offshore of the Georgia Bight can be seen penetrating offshore and possibly being entrained into the Gulf Stream. Chl-a in regions south of Jacksonville Florida and along the Carolina Capes is out of phase with Chl-a in the Georgia Bight. Such regional differences suggest Chl-a behaves differently from SST as it responds more directly to nutrient delivery than to wind forcing. The Georgia Bight traditionally gets nutrients from river runoff, such that increased nutrient content from elevated spring river runoff can stimulate a spring bloom of phytoplankton. Coastal areas near the Florida Straits gain most of their nutrients from Gulf Stream subsurface intrusions, which penetrate onto the shelf where isobaths diverge north of Cape Canaveral. Further downstream, nutrients exit off the shelf north of the Carolina Capes region, where isobaths converge [*Yoder et al.*, 1985]. Transport of GS-originating nutrients is facilitated by wind forcing. Persistent upwelling favorable wind may enhance nutrients onshore transport, fueling the growth of coastal phytoplankton, and thus increasing Chl-a concentration from June to September south of Cape Canaveral and north of the Carolina Capes. With subsurface Chl-a and nutrient data, it will be possible to better quantify the role of anomalous wind in coastal chlorophyll variation in summer, 2003.

5. Summary and Conclusion

[18] Concurrent MODIS SST and Chl-a data are used with a new analysis method DINEOF to produce daily, 4-km, cloud-free SST and Chl-a fields for the SAB in 2003. Compared to a traditional OI method, DINEOF is much more efficient in handling a large dataset. More importantly, the spatial and temporal correlation scales are computed internally in DINEOF, a perfect feature to apply to a complex coastal ocean such as the SAB, where a priori information about temporal and spatial decorrelation scales is not available. While no in situ Chl-a data were available, favorable comparisons between in situ observed SST and DINEOF SST results show the reconstruction is robust and successful. The complete 2003 cloud-free SST and Chl-a analyses, along with raw input data, are available online at: http://omglnx2.meas.ncsu.edu/travis/DINEOF.html.

[19] We analyzed the intrinsic linkages between the year-long daily, cloud-free SST and Chl-a analyses and high-resolution NARR wind fields. EOF analysis showed that the top two modes of surface wind have persistent upwelling favorable conditions from June to September. The first SST mode was due to the seasonal solar heating cycle. The second SST mode showed continued decrease along the SAB coast from June to September, a direct response to upwelling-favorable wind. The Chl-a EOFs did not show clear variations that can be directly attributed to wind forcing, but the regional out-of-phase characteristics identified by previous works were well re-created. Our analysis suggests Chl-a responded more directly to nutrient delivery from local river runoff and deep-ocean/GS upwelling. Surface winds may indirectly influence regional Chl-a distribution via modulating cross-shelf nutrient transport.

[20] Future work includes applying the DINEOF method to the entire MODIS data record and sub-regional areas to further highlight spatial patterns and the associated PCs. The resulting multiple-year cloud-free SST and Chl-a analyses will allow for studying their inter-annual variability on the SAB. Accompanying coupled bio-physical modeling work is ongoing. DINEOF reconstruction will provide a critical dataset for model validation and interpretation. Models in turn will provide subsurface information.

[21] **Acknowledgments.** We are grateful for the research support NASA provided through grant NNX07AF62G. We thank NASA GSFC, NCEP NARR, NOAA NDBC for providing data used in this study. We also thank anonymous reviewers for their constructive comments.

References

Alvera-Azcarate, A., A. Barth, M. Rixen, and J.-M. Beckers (2005), Reconstruction of incomplete oceanographic data sets using empirical orthogonal functions: Application to the Adriatic Sea Surface Temperature, *Ocean Modell.*, *9*, 325–346.

Alvera-Azcarate, A., A. Barth, J.-M. Beckers, and R. H. Weisberg (2007), Multivariate reconstruction of missing data in sea surface temperature, chlorophyll, and wind satellite fields, *J. Geophys. Res.*, *112*, C03008, doi:10.1029/2006JC003660.

Aretxabaleta, A., J. R. Nelson, J. O. Blanton, H. E. Seim, F. E. Werner, J. M. Bane, and R. Weisberg (2006), Cold event in the South Atlantic Bight during summer of 2 003: Anomalous hydrographic and atmospheric conditions, *J. Geophys. Res.*, *111*, C06007, doi:10.1029/2005JC003105.

Aretxabaleta, A., B. O. Blanton, H. E. Seim, F. E. Werner, J. R. Nelson, and E. P. Chassignet (2007), Cold event in the South Atlantic Bight during summer of 2003: Model simulations and implications, *J. Geophys. Res.*, *112*, C05022, doi:10.1029/2006JC003903.

Atkinson, L. P. (1985), Hydrography and nutrients of the Southeastern U.S. Continental Shelf, in *Oceanography of the Southeastern U.S. Continental Shelf*, *Coastal Estuarine Sci.*, vol. 2, edited by L. P. Atkinson et al., pp. 77–92, AGU, Washington, D. C.

Blanton, J. O., F. B. Schwing, A. H. Weber, L. J. Pietrafesa, and D. W. Hayes (1985), Wind stress climatology in the South Atlantic Bight, in *Oceanography of the Southeastern U.S. Continental Shelf*, *Coastal Estuarine Sci.*, vol. 2, edited by L. P. Atkinson et al., pp. 10–22, AGU, Washington, D. C.

He, R., and R. H. Weisberg (2003), West Florida Shelf circulation and temperature budget for the 1998 fall transition, *Cont. Shelf Res.*, *23*, 777–800.

He, R., R. H. Weisberg, H. Zhang, F. E. Muller-Karger, and R. Helber (2003), A cloud-free, satellite-derived, sea surface temperature analysis for the West Florida Shelf, *Geophys. Res. Lett.*, *30*(15), 1811, doi:10.1029/2003GL017673.

Lee, T. N., J. Yoder, and L. Atkinson (1991), Gulf Stream frontal eddy influence on the productivity of the southeast U.S. Continental Shelf, *J. Geophys Res.*, *96*, 22,191–22,205.

McClain, C. R., L. J. Pietrafesa, and J. A. Yoder (1984), Observations of Gulf Stream-induced and wind-driven upwelling in the Georgia Bight using ocean color and infrared imagery, *J. Geophys. Res.*, *89*, 3705–3723.

Schwing, F. B., and M. H. Pickett (2004), Comment on "Anomalous cold water detected along Mid-Atlantic Coast," *Eos Trans. AGU*, *85*, 554.

Signorini, S. R., and C. McClain (2006), Remote versus local forcing on chlorophyll variability in the South Atlantic Bight, *NASA Tech. Memo. TM-2006–214145*.

Signorini, S. R., and C. R. McClain (2007), Large-scale forcing impact on biomass variability in the South Atlantic Bight, *Geophys. Res. Lett.*, *34*, L21605, doi:10.1029/2007GL031121.

Yoder, J. A. (1985), Environmental control of phytoplankton production on the Southeastern U.S. Continental Shelf, in *Oceanography of the Southeastern U.S. Continental Shelf*, *Coastal Estuarine Sci.*, vol. 2, edited by L. P. Atkinson et al., pp. 93–103, AGU, Washington, D. C.

Yuan, D. (2006), Dynamics of the cold-water event off the southeast coast of the United States in the summer of 2003, *J. Phys. Oceanogr.*, *36*, 1912–1927.

R. He, M. Li, and T. N. Miles, Department of Marine, Earth and Atmospheric Sciences, North Carolina State University, Raleigh, NC, USA. (rhe@ncsu.edu)